

# NANOCOBALT OXIDE FOR THE ADSORPTION OF RARE EARTH ELEMENTS {LA(III) & ND(III)} - ADSORPTION ISOTHERMS AND KINETICS

<sup>1</sup>Dasari Vasundhara, <sup>2</sup>Vadivelu Anantha Lakshmi, <sup>3</sup>Duvvuri Suryakala

<sup>1,2</sup> Research Scholars, Department of Chemistry, GITAM Institute of Science, GITAM (deemed to be) University, Visakhapatnam-530045, Andhra Pradesh, India.

<sup>3</sup> Assistant Professor, Department of Chemistry, GITAM Institute of Science, GITAM (deemed to be) University, Visakhapatnam-530045, Andhra Pradesh, India. [duvzurisuryakala@gmail.com](mailto:duvzurisuryakala@gmail.com)

## ABSTRACT

Nano metal oxide ( $\text{Co}_3\text{O}_4$ ) is prepared efficiently in a simple, eco friendly and cost effective manner. Thermal decomposition of metal oxalates, which lead to transition metal oxide is considered to be a versatile method for the synthesis of transition metal oxide. Various characterization techniques like XRD, FTIR, SEM and EDS are applied to explore the morphology, bonding nature and size of the nano particle synthesized. Adsorption of rare earth elements {La(III) & Nd(III)} onto synthesized nanocobalt oxide is further studied using ICPAES method. The influencing parameters such as the adsorption efficiency, which include contact time, pH, initial concentration, and temperature, are studied. The adsorption isotherms, kinetics and thermodynamics are analyzed. It is observed that adsorption studies follow Pseudo second order kinetics and follow adsorption isotherms of Langmuir.

**KEYWORDS:** Nanocobalt oxide, Rare earth elements, Adsorption, ICPAES technique

## 1. INTRODUCTION

The surface area of crystalline materials increase with decrease in particle size, which increases the adsorption sites on the materials. Many metal oxides prepared by employing different synthetic routes [1-4], show excellent adsorption behavior. At room temperature pure form of cobalt is not stable as it can be converted to oxides like  $\text{CoO}$ ,  $\text{Co}_2\text{O}_3$ , and  $\text{Co}_3\text{O}_4$ . Among all  $\text{Co}_3\text{O}_4$  is the most stable phase and a P-type semiconductor, with high Young's modulus, which varies between 115 and 160 GPa. Normal crystal structure with occupation of tetrahedral sites by  $\text{Co}^{2+}$  and octahedral sites by  $\text{Co}^{3+}$  is exhibited by  $\text{Co}_3\text{O}_4$ . Magnetic moment is due to  $\text{Co}^{2+}$  ions largely because of spins, with a small contribution from spin-orbit coupling [5].

The nanopowder of cobalt oxide is extensively applied in gas sensor [6], magnetic [7], catalysis [8], lithium ion batteries [9], and electrochemical [10] depending on the structure, size, shape, and phase homogeneity and with surface morphologies. So much experimentation was done for the synthesis of cobalt oxide nanoparticles in past decades by using several well established techniques, like precipitation methods [11], thermal method [12], sonochemical method [13] and pyrolysis process [14]. In spite, these techniques have a limited control in particle functional properties and the yield is very less. Hence there is an acute need to find an alternative method and novel technique for the synthesis of nanoparticles that should be versatile, cost-effective and eco friendly.

Present work, we propose a simple, eco friendly cost effective method for metal oxalate preparation. This method is novel and simply pouring of one reaction solution into the other one, which is just sufficient for metal oxalate precipitation. Further thermal decomposition is carried out to obtain  $\text{Co}_3\text{O}_4$ , mesoporous metal oxides with a reasonable crystallinity.

Improper disposal of industrial effluent containing rare earth elements as well as various anthropogenic activities containing a wide range of potential contaminants pollutes water bodies results into toxicity to both human and aquatic life. REE form a coherent group and generally occur in the trivalent oxidation state [15].

There are various adsorbent materials (raw and modified) used for the removal of REEs from aqueous solutions such as, silica gel particles modified with acid groups [16], cysteine-functionalized chitosan magnetic nano-based particles [17], modified red clays [18], marine sediments [19] carbonized polydopamine nano carbon shells [20], granular hybrid [21].

Several methods including chemical precipitation, ion exchange, electro deposition, membrane separation etc. are applied to treat aqueous solutions containing rare earth elements. Among all these methods, chemical precipitation is considered the most economic one but is not sufficient for dilute solutions. Most well known techniques are Ion exchange and reverse osmosis, but they have rather, high cost and heavy maintenance subjected to fouling. To overcome this problem adsorption is one of the significant alternatives, particularly using low-cost natural sorbents like zeolites, agricultural wastes, biomass, seafood processing wastes, clay materials and natural waters [22].

ICP-AES occupies an invaluable position in the modern analytical laboratory due to its excellent sensitivity, simplicity, precision and accuracy and very limited interferences[23]. In the past, until time of the advent of ICP-AES, the determination of REE in geological samples was an expensive task and difficult and involving separation of the REE by utilizing time consuming methods like solvent extraction, ion exchange and precipitation, prior to analysis by techniques such as ICP-OES and XRF.

Here authors make an attempt to exploit meso porous  $\text{Co}_3\text{O}_4$  synthesized through thermal decomposition method as an adsorbent for the adsorption of REE in the form of La (III) & Nd (III) using ICPAES method. The adsorption isotherms and reaction kinetics are studied for the above mentioned systems.

## 2. EXPERIMENTAL DETAILS

Cobalt nitrate hexa hydrate  $\text{Co}(\text{NO}_3)_2 \cdot 6\text{H}_2\text{O}$  and Sodium oxalate ( $\text{Na}_2\text{C}_2\text{O}_4$ ), Lanthanum nitrate hexahydrate  $\text{La}(\text{NO}_3)_3 \cdot 6\text{H}_2\text{O}$  and Neodymium nitrate hexahydrate  $\text{Nd}(\text{NO}_3)_3 \cdot 6\text{H}_2\text{O}$  are used. All chemical reagents are commercial and of analytical grade, used directly without further purification. All the stock solutions are prepared from reagent grade compounds using double distilled water.

### Synthesis of nano mesoporous cobalt oxide:

The experimental approach for metal oxalate synthesis is discussed in detail. 100 mL of aqueous saturated sodium oxalate solution was added into a flask and stirred at room temperature. Then slowly 7.6 g of  $\text{Co}(\text{NO}_3)_2 \cdot 6\text{H}_2\text{O}$  was dissolved into 20 mL of water and then poured into the above sodium oxalate aqueous solution under continuous stirring. After fifteen minutes, the precipitates were collected by filtration and subsequently washed by distilled water and ethanol. Thereafter, the powder was dried at 80 °C overnight.

The synthesized metal oxide  $\text{Co}_3\text{O}_4$  is characterized using various analytical tools such as XRD, SEM-EDS, FTIR, and BET in order to obtain the size and various functional groups, elemental composition material characterization and surface area and porosity of the synthesized material.

## 3. RESULTS AND DISCUSSION

### Characterization of Nanometal oxides

The size and morphology and the of synthesized  $\text{Co}_3\text{O}_4$  nanoparticles are characterized by XRD, PAN analytical -X' Pert Pro X-ray diffraction instrument ; Cu Ka line ( $\lambda = 0.154 \text{ nm}$ ), FT-IR/Fourier Transform-Infra Red Spectroscopy (In the range of 400-4000  $\text{cm}^{-1}$  using KBr disc method), EDS –Energy Dispersive Spectroscopy , SEM/ scanning electron microscopy (The JEOL JSM-7600F FEG-SEM) and HR-TEM, high resolution transmission electron microscopy (HRTEM Jeol/JEM 2100) and BET.

### XRD of Nano metal oxides

The synthesized oxides  $\text{Co}_3\text{O}_4$  are structurally characterized by XRD, using the sample scanned from 10°-80° at a scanning rate of 0.4°/second. From Scherrer Equation (1), it was confirmed that the synthesized metal oxides  $\text{Co}_3\text{O}_4$  have the crystallite size of 30.22 nm. Figure 1 is well matched with the standard JCPDS file

Scherrer Equation, Crystallite size =  $0.9\lambda / B \cos \Theta$  .....(1)

Here  $\lambda$  = X-ray wavelength,

B = Full width at half maximum intensity of the peak

$\Theta$  = Bragg angle

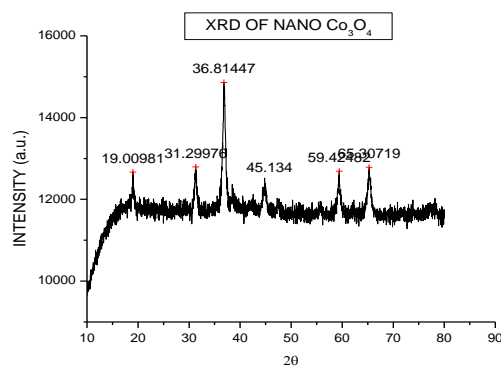


Figure1: XRD Patterns of nano $\text{Co}_3\text{O}_4$

### FT-IR Spectra of Nano metal oxides

The synthesized metal oxides  $\text{Co}_3\text{O}_4$  is characterized by FT-IR spectra shown in figure 2 is in the range of  $400\text{-}4000\text{ cm}^{-1}$  using KBr disc method. It is observed a stretching frequency at  $3422\text{ cm}^{-1}$  and a weak asymmetric band at  $1627\text{ cm}^{-1}$  support the presence of  $\text{OH}^-$  group due to the absorption of water by nanoparticle during sample preparation.

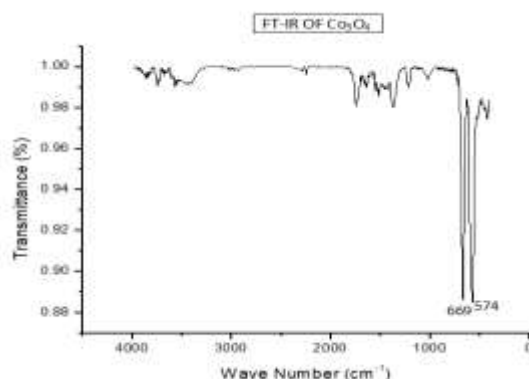


Figure2: FTIR of nano $\text{Co}_3\text{O}_4$

The presence of two strong M–O stretching and bending frequencies at  $669.69\text{ cm}^{-1}$  and  $574.74\text{ cm}^{-1}$ , respectively, supports the presence of phase purity with mono dispersity in the face centered cubic structure [12]. Generally nano materials absorb moisture from the environment, because of which low intensity peaks of  $\text{-OH}$  in the FT-IR spectra are observed.

#### SEM and EDS of Nano metal oxide

SEM-EDS. Figure 3 supports the microcrystalline nature of the particle after calcinations with least degree of agglomeration. Particles seem to have an irregular shape with chemical homogeneity with uniform morphology due to the presence of inter particle surface connectivity. It was observed that the annealing temperature increases the crystalline nature of the particle that changes due to nucleation [24,25]. The morphologies of the  $\text{Co}_3\text{O}_4$ , are in spherical structure whose dimensions are in nanometer scale.

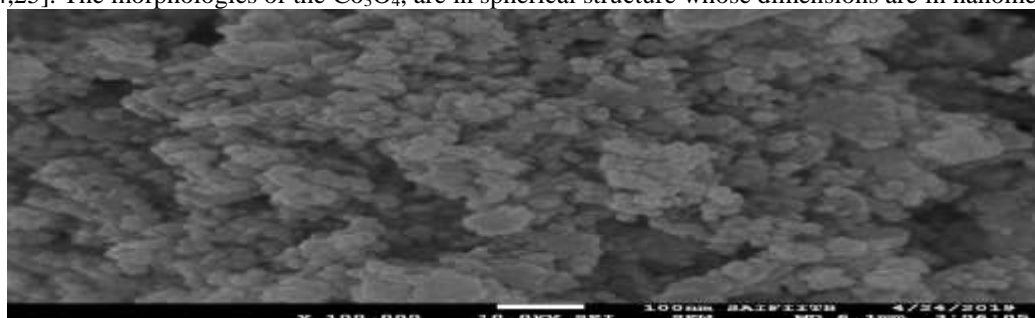


Figure3: SEM of nano  $\text{Co}_3\text{O}_4$

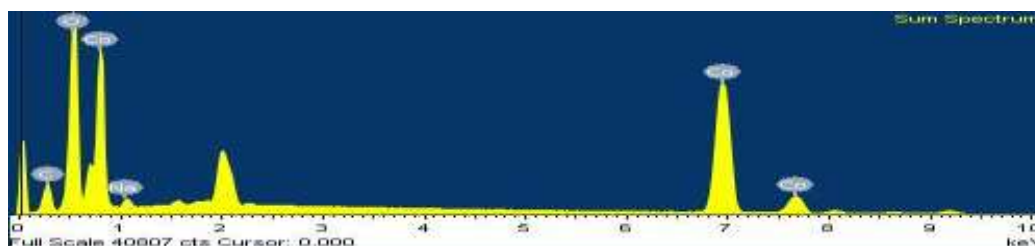


Figure 4 : SEM- EDS of nano  $\text{Co}_3\text{O}_4$

Table 1: Elemental Composition of  $\text{Co}_3\text{O}_4$

Element	App Conc.	Intensity Corrn.	Weight%	Weight% Sigma	Atomic%
C K	3.36	0.5229	7.49	0.11	19.91
O K	25.89	1.5214	19.83	0.08	39.58
Na K	0.59	0.5245	1.32	0.04	1.83
Co K	56.05	0.9148	71.37	0.12	38.68
Totals			100.00		

### BET analysis

Brunauer – Emmett – Teller (BET) analysis was employed for exploring the specific surface area and porosity. Here the material is chilled to liquid nitrogen hotness and depicted to a nitrogen (gas) adsorbent. The BET surface area of nanoCo<sub>3</sub>O<sub>4</sub> is measured to be 88.37 m<sup>2</sup>g<sup>-1</sup>.

### Batch adsorption study

Another important objective of this work is to adsorb REEs such as La(III) and Nd(III) from aqueous solutions using Co<sub>3</sub>O<sub>4</sub> nano particles using ICPAES technique. Several experimental parameters like initial dye concentration, adsorbent dose, contact time, solution pH and temperature can affect the extent of removal of REE. Several batch adsorption studies were conducted at 313K. The adsorption studies are done to investigate the variation of REE strength, nano particles amount (1to30 ppm) and temperature (293,303,313,323K). The experiments were conducted by varying one of the parameter while keeping other factors fixed. After fixed intervals of time (10min) the strength of the dye was monitored by applying ICP-AES technique.

### Effect of pH

Solution pH is a crucial feature in operating the adsorption capability of REE on to adsorbent (nanoCo<sub>3</sub>O<sub>4</sub>). Figure 5 describes the percentage removal of La(III) and Nd(III) vs Co<sub>3</sub>O<sub>4</sub> at various pH values. Various pH ranges acidic, neutral and basic are used for adsorption studies. Graph shows that the pH of the both REE is “6.5” for the optimum adsorption on to the prepared Co<sub>3</sub>O<sub>4</sub> nano particles. Hence acidic pH is preferred for further the batch adsorption studies

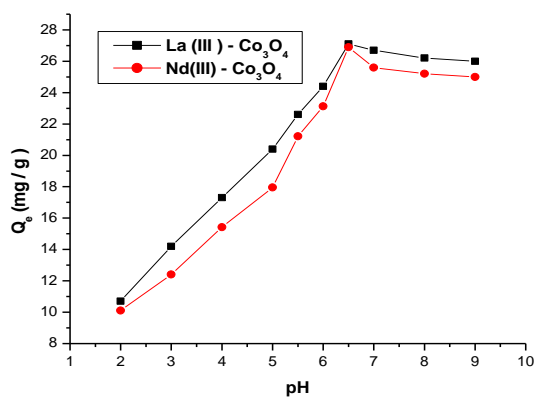


Figure 5: Effect of P<sup>H</sup> on adsorption of La(III) and Nd( III) on nano Co<sub>3</sub>O<sub>4</sub> particles at 313K

### Effect of contact time

Several batch adsorption studies are conducted for REE {La(III) and Nd(III)} in the concentration limit from 1 - 30 mg/L on Co<sub>3</sub>O<sub>4</sub> nano particles respectively. The quantity of REE being removed on the surface of nano structures enhances on increasing time of contact till a plateau is reached. This explains the dynamic equilibrium state of the REE, where the quantity adsorbed on to the adsorbent Co<sub>3</sub>O<sub>4</sub> is in equilibrium with that of rare earth element in the solution. At 40 minutes the equilibrium is observed for both the REE on Co<sub>3</sub>O<sub>4</sub> nano particles. The mechanism explains the confirmation of pollutant molecules to the outer layer before the dispersal on to the surface of adsorbent and then completely entry in to the permeable arrangement of nano structures.

There is repulsion or electrostatic hindrance among the adsorbed effluent on to the adsorbent surface. Finally on increasing, effluent strength, the quantity of pollutant adsorbed for every part (quantity) of Co<sub>3</sub>O<sub>4</sub> (unit adsorption capability) enhances, while it decreases with increment in the adsorbent dosage because of unsaturation of adsorption sites.

### Effect of adsorbent mass

Adsorption studies were carried to know about the outcome of adsorbent amount on removal of La(III) and Nd(III) on changing the quantity of adsorbent in the limits for fixed concentration of REE at constant temperature of 313K. On enhancing the adsorbent

amount from 5- 20mg, adsorption percentage enhanced along less equilibrium time. The existing places on the adsorbent became restricted at higher concentration, and hence no additional adsorption, which could be explained with enhanced surface area, abundant sites for adsorption. The quantity of adsorbent mass is observed to be 10 mg for removal of La(III) and Nd(III) respectively.

**Influence of initial dye concentration**

REE concentration influences in the removal of effluent by nano particles at the pH value of 6.5 value at 313K is shown in figure 6 and figure 7 respectively. The pollutant concentration used in the experiment was 1 to 30 mg L<sup>-1</sup>. At lower concentrations the effluent material in solution reside in binding locations those are available on adsorbent. This grades an appropriate adsorption. The concentration of the REE was determined with various time intervals varying between 0 to 60 minutes. It is observed, the adsorption/removal of La(III) could be fast from the starting of the investigation and at the end, reached to equilibrium. Similar trend is observed in Nd(III) also. From the above results equilibrium time was 40 min, fixed throughout the experiment.

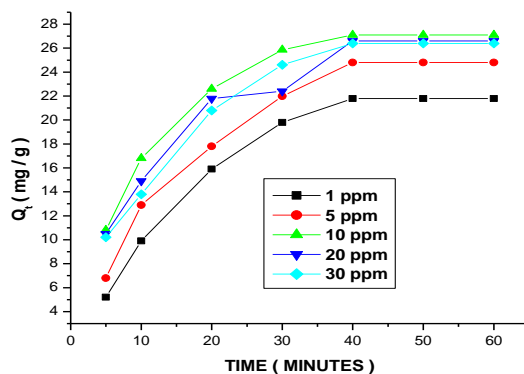


Figure 6: Effect of REE, La(III) on adsorption onto nano Co<sub>3</sub>O<sub>4</sub> at 313 K

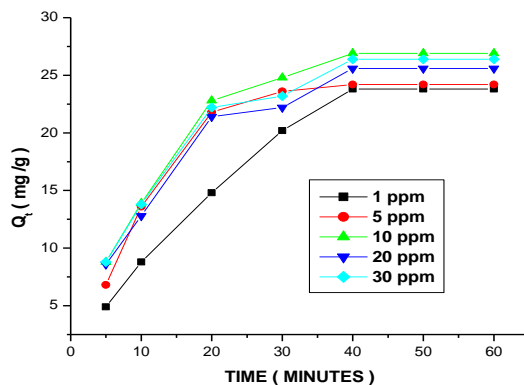


Figure 7: Effect of REE, Nd(III) on adsorption onto nano Co<sub>3</sub>O<sub>4</sub> at 313 K

**Langmuir adsorption isotherm**

This isotherm explains the adsorption is appropriate near homogeneous phases, and is specific on the surface of adsorbent which is observed to be monolayer. The linear Langmuir isotherm model is given as

$$\frac{C_e}{q_e} = \frac{1}{K_L Q_0} + \frac{C_e}{Q_e} \dots\dots\dots(2)$$

Where the terms represent their own words. The important properties of Langmuir isotherm is explained by a fixed numerical value which is dimensionless and known as equilibrium parameter R<sub>L</sub>.

$$R_L = \frac{1}{(1+K_L C_0)} \dots\dots\dots(3)$$

The rate of R<sub>L</sub> expresses the behavior of Langmuir isotherm, which is irreversible (R<sub>L</sub>= 0), favorable at conditions of 0 < R<sub>L</sub>< 1, and Linear at R<sub>L</sub>= 1 or not favorable at R<sub>L</sub>> 1.

**Table 2** Langmuir adsorption isotherms values for the adsorption of La(III) and Nd(III) on nano Co<sub>3</sub>O<sub>4</sub>

Isotherm Model	Parameter	La(III)	Nd(III)
Langmuir	$Q_{max}$ (mg/g)	27.2479	26.2550
	$K_L$ (L/mg)	1.0397	1.2476
	$R^2$	0.9960	0.9999

Figure 8 and Figure 9 represents the Langmuir isotherms of La(III) and Nd(III) by the adsorption onto  $Co_3O_4$  nano particles.

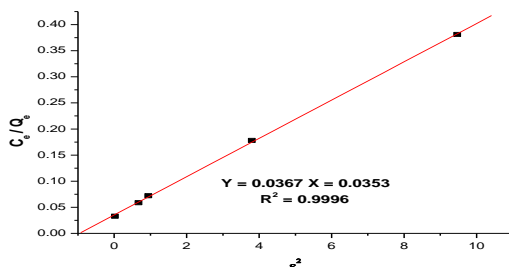


Figure 8: Langmuir adsorption isotherm in the adsorption of La (III) on nano  $Co_3O_4$

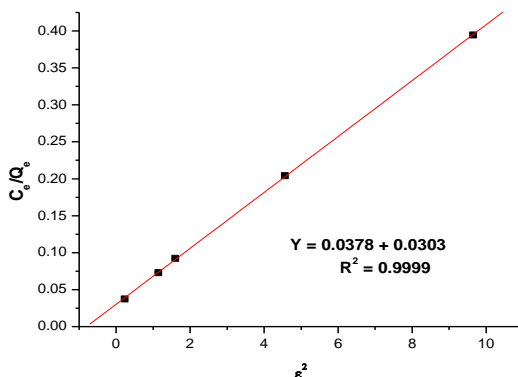


Figure 9: Langmuir adsorption isotherm in the adsorption of Nd (III) on nano  $Co_3O_4$

The experimental value is in correlation with graphical value of  $Q$  for both REEs. From the result it is observed the  $Co_3O_4$  nano particle has better adsorption capacity over the selected REEs.

**Adsorption kinetics**

The adsorption procedure is normally quick instead of inner and outside dissemination. But in elaboration, adsorption equilibrium time proposes that the interior dispersion manages the response rate. In this context the adsorption of effluent was applied to PFO and PSO expressions in evaluating the kinetics of adsorption technique. The result of the adsorption kinetics was gained for proposed REEs. The issues are observed in table 3. The adsorption kinetic plots for pseudo second order kinetics can be presented in figure 10 and 11 . Usually the correlation coefficient ( $R^2$ ) value is the base and from which best fit can be selected. The linear formula of the Pseudo second order kinetic model equation can be presented

$$\frac{t}{q_t} = \frac{1}{K_2 q_e} + \frac{t}{q_e} \dots\dots\dots(4)$$

$q_t$  (mg/g) = adsorbate strength at a given time  $t$ ,  $q_e$  (mg/g) = strength of adsorbate at equilibrium,  $K_2$  (g/mg min) = PSO rate constant. The linear graph of  $t/q_t$  vs ‘ $t$ ’ can pursue the data of  $q_e$ ,  $K_2$  from the slope, intercept correspondingly. From the observation, the correlation coefficient values are nearly ideal. This indicates a better conformity with experimental, theoretical values. Furthermore better correlation is established among  $q_e$  values determined applying PSO model and experimental investigation.

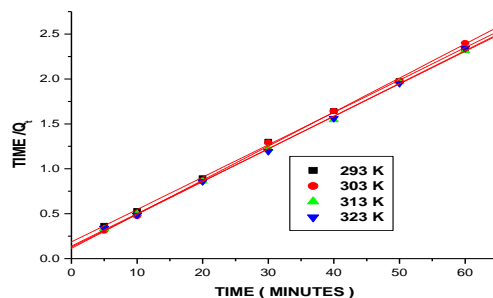


Figure 10: PSO kinetic model for the adsorption of La(III) on nanoCo<sub>3</sub>O<sub>4</sub>

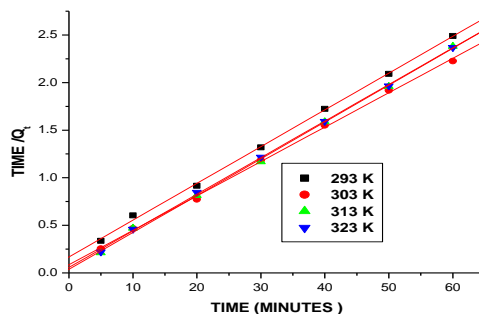


Figure 11: PSO kinetic model for the adsorption of Nd(III) on nanoCo<sub>3</sub>O<sub>4</sub>

Table 3 Pseudo second order values for the adsorption of La(III) and Nd(III) on nano Co<sub>3</sub>O<sub>4</sub>

Dyes	Q cal	Qobs	K <sub>2</sub>	R <sup>2</sup>
La(III)	27.1	27.7008	0.0093	0.9994
Nd(III)	26.9	25.8339	0.0038	0.9989

Hence from Table 3. Pseudo second order model best fit into the kinetics.

#### 4. CONCLUSION

From the above results and discussion it is understood that Co<sub>3</sub>O<sub>4</sub> nano particles are successfully prepared and applied in the adsorption of rare earth elements like Lanthanum and Neodmium. ICPAES technique is applied for the entire study and factors effecting like pH, initial concentration of adsorbate, adsorbent, contact time are also investigated. The study extended to explore the feasibility of the reaction. The pseudo second order kinetics best fit into the model. Hence nanoCo<sub>3</sub>O<sub>4</sub> is considered to be better adsorbents in the adsorption of rare earth elements.

#### 5. REFERENCES

1. T.S. Towle, J.R. Bargar, G.E. Brown, G.A. Parks, *J. Colloid. Interf. Sci* **1997**, 187 62-68.  
J.R. Bargar, S.N. Towle, J.G.E. Brown, G.A. Parks, *J. Colloid. Interf. Sci.* **1997**, 185, 473-478.
2. J.R. Bargar, G.E. Brown, G.A. Parks, *Geochimica. Acta* **1997**, 61, 2617-2621.
3. A. Lagashetty, H. Vijayanand, S. Basavaraja, N.N. Mallikarjuna and A. Venkataraman, *Bull. Mater. Sci.* **2010**, 33(1), 1-6.
4. I Prasetyo, N.I. FMukti, M. Fahrurrozi, T. Ariyanto, *Asean J. Chem. Eng.* **2018**, 18, 9-16.
5. W.Y. Li, L.N. Xu, J. Chen, *Adv. Func. Mat.* **2005**, 15 (5), 851-857.
6. L. Zhang, D. Xue, *J of Mat Sci Lett*, **2002** 21, (24), 1931-1933.



7. X.Xie ,W.Shen, *Nanoscale*, **2009**, 1, 50–60.
8. H.Qiao,L.Xiao,Z.Zheng,H.Liu,F.Jia,L.Zhang,*Journal of Power Sources*,2008,185,(1), 486–491.
9. H.J.Guo,Q.M.Sun,X.H.Li,Z.X.Wang,W.J.Peng,*Transactions of NonferrousMetals Society of China*, **2009**.19,(2),372–376.
10. V.Srinivasan,J.W.Weidner,*Journal of Power Sources* **2002**,108, (1-2),15–20.
11. M.Salavati-Niasari,N.Mir,F.Davar,*Journal of Physics and Chemistry of Solids*, **2009**.70(5), 847–852.
12. K.H.Kim,K.B.Kim, *Ultrasonics Sonochemistry*, **2008**,15(6),1019–1025.
13. D.Srikala,V.N.Singh,A.Banerjee,B.R.Mehta,S.Patnaik,*Journal of Nanoscience and Nanotechnology*, **2009**, 9(9), 5627–5632.
14. R.T.Shannon, *Acta Crystallogr. Sect. A Cryst. Phys. Diffr. Theor. general Crystallogr.* **1976**, 32 (5),751–767.
15. T.Ogata,H.Narita,M.Tanaka, *Hydrometallurgy*,**2015**,152,178–182.
16. A.A.Galhoum,M.G.Mafhouz,S.T. Abdel-Rehem, N.A. Gomaa, A.A. Atia, T. Vincent, E. Guibal, *Nanomaterials* **2015**,5,154–179.
17. A.Gładysz-Płaska,M.Majdan,E.Grabias,*J.Radioanal. Nucl. Chem.***2014**, 301,33–40.
18. I.Liatsou,M.Efstathiou,I Pashalidis, *J. Radioanal. Nucl. Chem.* **2015**,304,41–45.
19. S.Xiaoqi,L.Huimin,S.M.Mahurin,L.Rui,H.Xisen,D.Sheng, *J.Rare Earths* **2016**,34,77–82.
20. Y.Zhu,Y.Zheng,A.Wang, *J. Environ. Chem. Eng.* **2015**,3,1416–1425.
21. D.Martínez-Romero,G.Bailén,M.Serrano,F.Guillén,J.M.Valverde,P.Zapata,S.Castillo,
22. D.Valero, *Crit. Rev. Food Sci. Nutr.***2007**,47,543–560.
23. V. Balaram, K.V. Anjaiah, M.R.P.Reddy, *Analyst*, **1995**,120, 1401-1406.
24. Q. Yuanchun, Z. Yanbao, W. Zhishen, *Materials Chemistry and Physics*, **2008**, 110,(2- 3),457–462.
25. J. H. Smatt, B.Spliethoff, J.B.Rosenholm,M.Linden, *Chemical Communications*,
26. **2004**,10 (19), 2188–2189.